

Soliton ratchets induced by ac forces with harmonic mixing

Mario Salerno[†] and Yaroslav Zolotaryuk[‡]

[†] *Dipartimento di Fisica “E. R. Caianiello” and Istituto Nazionale di Fisica della Materia (INFM),
Università di Salerno, I-84081 Baronissi, Salerno, Italy*

[‡] *Section of Mathematical Physics, IMM, Technical University of Denmark,
DK-2800, Kgs. Lyngby, Denmark*

(November 17, 2018)

The ratchet dynamics of a kink (topological soliton) of a dissipative sine-Gordon equation in the presence of ac forces with harmonic mixing (at least bi-harmonic) of zero mean is studied. The dependence of the kink mean velocity on system parameters is investigated numerically and the results are compared with a perturbation analysis based on a point particle representation of the soliton. We find that first order perturbative calculations lead to incomplete descriptions, due to the important role played by the soliton-phonon interaction in establishing the phenomenon. The role played by the temporal symmetry of the system in establishing soliton ratchets is also emphasized. In particular, we show the existence of an asymmetric internal mode on the kink profile which couples to the kink translational mode through the damping in the system. Effective soliton transport is achieved when the internal mode and the external force get phase locked. We find that for kinks driven by bi-harmonic drivers consisting of the superposition of a fundamental driver with its first odd harmonic, the transport arises only due to this *internal mode* mechanism, while for bi-harmonic drivers with even harmonic superposition, also a point-particle contribution to the drift velocity is present. The phenomenon is robust enough to survive the presence of thermal noise in the system and can lead to several interesting physical applications.

PACS numbers: 05.45.-a, 05.60.Cd, 05.45.Ac

Transport phenomena based on nonlinear effects are at the heart of many problems in physics [1]. In this context it was generally believed that an ac force of zero mean cannot lead to directed nonzero currents. Recent studies of the so called *ratchet effect* have shown that this belief was wrong [2]. A ratchet system can be described as a Brownian particle in an asymmetric periodic potential, moving in a specific direction in presence of damping, under the action of ac forces of zero average. The origin of a net motion is associated to the breaking of the space-temporal symmetries of the system [3,4], leading to the de-symmetrization of Lévy flights [for Hamiltonian systems] [5] and to phase locking phenomena between the particle motion and the external driving force [6,7].

This effect has a number of applications in various branches of physics and biology and is believed to be the basic mechanism for the functioning of biological motors (see reviews [2] and references therein). The ratchet effect, originally studied for Brownian particles, was generalized to dynamical systems [8] and to partial differential equations (PDE) of soliton type, mainly in the over-damped regime [9], or with asymmetric potentials [10–14]. In the over-damped case, the damping in the system suppress all the degrees of freedom associated with the background radiation so that soliton ratchets become very similar to point particle ratchets. For under-damped or moderately damped systems, however, the situation is quite different since the radiation field can interact with the soliton and influence the transport. Under-damped soliton ratchets in asymmetric potentials and driven by sinusoidal forces, were recently investigated in

Refs. [13,14]. In particular, in Ref. [13] the basic mechanism underlying the phenomenon was identified in the existence of an asymmetric internal mode which couples, through the damping in the system, to the soliton translational mode. Effective transport was found when the internal mode and the external force were phase locked. Moreover, it was shown that the effect of soliton transport decreases with increase of the damping, the maximal transport being achieved in the under-damped regime.

On the other hand, it is known that for point particle ratchets transport phenomena are possible also in symmetric periodic potentials, provided the driving force breaks suitable temporal symmetries of the system (i.e. the ones which relates orbits of opposite velocities in phase space [15]). Since in concrete applications it is more easy to act on the temporal part (by using external forces) than on the spatial part (by inducing distortion of the potential) of a system, it is interesting to explore the above possibility also in soliton systems.

The present paper is just devoted to this problem. More precisely, we show that topological solitons of nonlinear PDEs with symmetric potentials can acquire finite drift velocities in the presence of bi-harmonic forces of zero average consisting of the superposition of two harmonics, the fundamental and one of its overtones (harmonic mixing drivers). Bi-harmonic forces were used in the literature to suppress chaos in dynamical systems and in soliton equations [16], as well as, to control the transport properties of single particle ratchets [7]. In the present paper we demonstrate, on the particular example of the sine-Gordon system, that bi-harmonic driv-

ing forces with certain symmetries can be effective to create soliton ratchets. The phenomenon is investigated both numerically, by direct simulations, and analytically, using symmetry considerations and soliton perturbation theory. We show that a first order perturbation analysis of the soliton dynamics captures only the qualitative features of the phenomenon, leading to poor quantitative agreements with numerical results. The reason of this discrepancy is ascribed to the soliton-phonon interaction which is obviously missing in a point-particle description (it arises only at the second order in the perturbation expansion [17]).

In general the situation can be described as follows. Besides a point particle contribution to the drift velocity there is an equally important contribution coming from the soliton-phonon interaction. This last manifests itself with the appearance of an internal oscillation on the soliton profile, asymmetric in space, which induces a net motion in a similar manner as described in Ref. [13]. In particular we show that this oscillation can be phase locked to the external driving force and can couple to the kink translational mode, through the damping in the system. The energy, “pumped”, by the ac field into the internal mode is then converted by the above mechanism into net motion of the kink. Internal oscillations on anti-kink profiles have opposite asymmetry compared to kinks, so that kink and anti-kink ratchets give rise to motion in opposite directions.

The dependence of the phenomenon on system parameters such as the damping in the system, frequency, amplitudes, relative phase of the bi-harmonic driving force, as well as, on the presence of white noise in the system, is investigated by means of direct numerical integrations of the sine-Gordon equation. The interaction of soliton ratchets with the boundaries of a finite system is also investigated. For reflecting edges we find that, depending on the initial velocity and position of the kink, the ratchet dynamics can be either destroyed or reflected as an anti-kink ratchet moving in the opposite direction. These results could be important for applications to physical systems such as long Josephson junctions, as we briefly discuss at the end of the paper.

The paper is organized as follows. In Section I we investigate the dynamics of the perturbed sine-Gordon equation, as a model for soliton ratchets in presence of asymmetric forcing and damping, both in terms of symmetry arguments and first order perturbation theory. In Section II we study soliton ratchets by direct numerical integrations of the perturbed sine-Gordon system and provide a consistent interpretation of the phenomenon. Qualitative and quantitative features of soliton ratchets are compared with the predictions of the first order perturbation analysis. The phenomenon is investigated in the deterministic case (i.e. in absence of noise) and in presence of a white noise term in the system. We find that the soliton ratchets are robust enough to overcome the presence of small amplitude noises, this making them of interest for practical applications. In Section III the

interaction of soliton ratchets with system boundaries is considered, while in Section IV we summarize the main result of the paper and discuss possible applications of the phenomenon.

I. MODEL ANALYSIS

Direct soliton motion induced by ac signals have been investigated in the literature mainly for ac forces with single-harmonic content [18]. As well known, for symmetric field potentials this situation does not lead to soliton ratchet dynamics. To this regard we remark that the dc motion observed for a sine-Gordon kink driven by single harmonic forces in absence of damping [19], and its generalization to the case of small damping [20], as well as, dc motion obtained from spatially-inhomogeneous drivers [21], should not be confused with soliton ratchets. In these cases, indeed, the dc motion strongly depends on the initial conditions and quickly disappears as the damping in the system is increased. On the contrary, soliton ratchets do not depend on initial conditions and exist also for relatively higher damping. We remark that net soliton motion independent on initial conditions, can be induced by the mixing of an additive and a parametric (single harmonic) driver as shown in Ref. [22] for solitons of the ϕ^4 model.

In this section we shall investigate soliton ratchets in symmetric potentials driven by periodic bi-harmonic forces of zero mean. As a working model we take the following perturbed sine-Gordon equation

$$u_{tt} - u_{xx} + \sin u = -\alpha u_t - E(t) + n(x, t) , \quad (1)$$

with α denoting the damping coefficient, $n(x, t)$ a white noise term with autocorrelation

$$\langle n(x, t)n(x', t') \rangle = D\delta(x - x')\delta(t - t') , \quad (2)$$

and $E(t)$ a driver of the form

$$E(t) = E_1 \cos \omega t + E_2 \cos (m\omega t + \theta) , \quad (3)$$

(the case $E_2 \neq 0$ is referred to as *bi-harmonic driver* with even or odd harmonic mixing, depending on m being even or odd). Note that although the symmetry properties of this driver are reduced if $E_2 \neq 0$ and $\theta \neq 0 \pmod{\pi}$, the force is periodic, with period $T = 2\pi/\omega$, and has zero mean (the analysis can be generalized to more harmonic components and to arbitrary non-sinusoidal periodic forces). The unperturbed version of Eq. (1) [the perturbation being $\epsilon f(t) \equiv -E(t) - \alpha u_t(x, t)$] is the well known sine-Gordon equation with exact soliton (kinks, anti-kinks) solutions which depend on a free parameter, the velocity v of the kink, which lies in the range $-1 < v < 1$.

It is of interest to investigate the conditions under which a bi-harmonic driver of type (3) can induce soliton ratchets in Eq. (1). To this end we remark that due

to the translational invariance of the sine-Gordon system (we assume an infinite system or a finite one with periodic boundary conditions) we have that to each soliton trajectory with velocity v there is a specular trajectory with the velocity $-v$. One can expect that, in analogy with single particle ratchets [15], only forces which break the $v \rightarrow -v$ symmetry should induce net motion. This argument can be formalized in terms of the kink velocity

$$v = \frac{1}{2\pi} \int_{-\infty}^{+\infty} x u_{xt} dx , \quad (4)$$

as follows (note that one could use the momentum of the kink as well, instead of the velocity). Among the possible shifts and reflections in t, x and u , we identify the symmetry operations which change the sign of v keeping the sign of the topological charge

$$Q = \frac{1}{2\pi} \int_{-\infty}^{+\infty} u_x dx , \quad (5)$$

unchanged (this means that we avoid kink anti-kink transformations). It is easy to check that there is only one symmetry transformation which changes the sign of kink velocity and leaves the equation of motion unchanged, i.e.

$$x \rightarrow -x + x_0 , \quad t \rightarrow t + \frac{T}{2} , \quad u \rightarrow -u + 2\pi . \quad (6)$$

This holds true for driving fields satisfying the following condition

$$E(t + T/2) = -E(t) . \quad (7)$$

We remark that the above symmetry argument accounts only for the breakage of the $v \rightarrow -v$ point-particle symmetry of the soliton, ignoring possible contributions coming from the soliton-phonon interaction [23]. From Eq. (3) we see that condition (7) is always satisfied for drivers with odd mixing while it is always broken for drivers with m even (obviously we take $E_2 \neq 0$). Thus, the $v \rightarrow -v$ symmetry predicts that a sine-Gordon soliton should exhibit a ratchet dynamics when driven by a $m = 2$ force (one needs to break the symmetry (7) to get the drift motion), but not when driven by a $m = 3$ force.

To the same conclusion one can arrive also from first order perturbation theory, taking as collective coordinate ansatz for the kink profile

$$u(x, t) = 4 \arctan \left(\exp \left[\frac{x - X(t)}{\sqrt{1 - \dot{X}^2(t)}} \right] \right) . \quad (8)$$

An ordinary differential equation (ODE) for kink's center of mass $X(t)$, can be readily obtained by differentiating the momentum (see Refs. [19,24]),

$$P = - \int_{-\infty}^{+\infty} \phi_x \phi_t dx , \quad (9)$$

with respect to time, and using Eq. (1) and ansatz (8) to simplify the expression. This leads to

$$\frac{dP}{dt} = -\alpha P + 2\pi E(t) , \quad (10)$$

or equivalently

$$\dot{v} = -\frac{1}{4}(1 - v^2) \left[-\pi \sqrt{1 - v^2} E(t) + 4\alpha v \right] , \quad (11)$$

where $v(t) = \dot{X}(t)$ and we assumed the usual relativistic relation $P(t) = 8v(t)/\sqrt{1 - v(t)^2}$ between velocity and momentum to be valid for all times. Equation (10) can be readily solved for $P(t)$, from which the kink velocity can be obtained as

$$v = \frac{P(t)}{8\sqrt{1 + \frac{P^2(t)}{64}}} . \quad (12)$$

From this equation an analytical expression of the average kink velocity

$$\langle v \rangle = \frac{\omega}{2\pi} \int_0^T v(t') dt' , \quad T = \frac{2\pi}{\omega} , \quad (13)$$

valid in the limit $E_j/\sqrt{\alpha^2 + (j\omega)^2} \ll 1$, $j = 1, 2$, (i.e. small momentums or small drift velocities), can be obtained for the case of $m = 2$, by expanding the square root in Eq. (12) in series, this giving

$$\langle v \rangle = \frac{3}{512} \frac{E_1^2 E_2 \pi^3}{(\alpha^2 + \omega^2) \sqrt{\alpha^2 + 4\omega^2}} \sin(\theta - \theta_0) , \quad (14)$$

$$\theta_0 = \arctan \left[\frac{\alpha(\alpha^2 + 3\omega^2)}{2\omega^3} \right] .$$

From this expression we see that the dependence of $\langle v \rangle$ on the relative phase is perfectly sinusoidal. Similar calculations for the $m = 3$ case show that the average kink velocity is zero independently on the value of the relative phase θ (as well as of an arbitrary initial phase).

These results can be easily understood from the effects of the symmetry properties of the force on the dynamics. In Fig. 1 the force $E(t)$, viewed as sequence of alternating pulses of equal intensities (i.e. with the same area under the curve) and indicated by dark and light fillings in the figure, is reported for the cases $m = 2, 3$. We see that for $m = 3$ these pulses perfectly balance so that no net motion can arise, while for $m = 2$ there is not such a balance (in both cases, however, the average of the force is zero).

In Fig. 2 we report the dynamics obtained from numerical integrations of Eq. (11) for the case $m = 2$. We also show the response of the system to the single dark and light pulses composing the force, from which we see that although these pulses have equal intensities, the answer of the system is quite different in the two cases. Note that the negative pulse is more effective than the

positive one to produce motion as one can see from the fact that the area under the negative trajectory is greater than the one generated by the positive pulse. This is obviously a consequence of the nonlinearity of the system (in a linear system the area under the two curves would just be the same). For the particular example of Fig. 2 (i.e. $\theta = 0$) one expects then that a net motion in the negative direction will exist. This is indeed what one finds from integrations of the perturbation equation (11) with $\theta = 0$ [see Fig. (4) below].

In Fig. 3 the motion of the kink center of mass, X , obtained from numerical simulations of Eq. (11) for the cases $m = 2, 3$, is also reported. We see that while a well defined drift velocity in the $m = 2$ case arises, no dc motion is present in the $m = 3$ case, this being in agreement with our symmetry analysis.

We also find that the average velocity in (13), computed after the system reached steady state regime, depends on the relative phase θ with a law which is well approximated by $\langle v \rangle = A \sin(\theta - \theta_0)$, with $A = 0.058$ and $\theta_0 = 0.8$. This is shown in Fig. 4 where the dependence of the average velocity on θ , as computed from Eq.(11), is reported with dots, while the continuous line represents the above approximating function. Note that, although the sinusoidal dependence is in perfect agreement with the approximate result in Eq. (14), the explicit values of A, θ_0 differ from those predicted by (14), these being respectively $A = 0.12, \theta_0 = 0.56$ (this is due to the fact that, for the chosen set of parameters, the approximation of small drift velocities is not valid).

We also note that from Eq. (14) the point-particle contribution to the drift velocity is expected to be cubic in the driver amplitudes, this implying that there could be equally important contributions to the soliton velocity at higher orders of the perturbation expansion. In particular, the interaction of the soliton with the phonons in the system, first appearing at second order [17], should not be overlooked. Although the development of a theory which includes second order effects is quite challenging, it is out of the purposes of the present paper. In the next section we shall instead resort to numerical simulations of Eq. (1) for a full investigation of the problem and compare the results with those predicted by the present section.

II. NUMERICAL STUDIES

To numerically investigate sine-Gordon soliton ratchets driven by bi-harmonic fields, we have used standard finite difference schemes to reduce Eq. (1) into a set of ODE which were then integrated in time with a 4th order Runge-Kutta method. To understand the basic mechanism underlying the phenomenon we shall first concentrate on the deterministic case by putting $n(x, t) = 0$ in Eq. (1), and then show that the results obtained in this case will survive in the presence of noise. In Fig.

5 the dynamics of a sine-Gordon kink, initially at rest, driven by a bi-harmonic driver with $m = 2$ and by a single harmonic driver (i.e. $E_2 = 0$), are reported in Figs. 5a,b, respectively (note that we use contour plots to show the time evolution surface generated by the kink profile). From these figures we see that, in the case $m = 2$ the soliton center of mass move with a constant drift velocity (note that the shape of the kink during the motion is highly distorted), while for the single harmonic driver, it oscillates around the initial position (periodic boundary conditions are used in the simulation). This demonstrates the importance of bi-harmonic drivers in establishing soliton ratchets.

In Fig. 6 we report the dynamics of an anti-kink ratchet, for the same parameters values as in Fig. 5. We see that, in analogy with soliton ratchets in spatially asymmetric potentials [9,10,13], anti-kinks ratchets move opposite to kinks, the absolute value of the drift velocity being the same.

To check the point particle perturbation analysis of the previous section, we have studied the dependence of kink's average velocity on system parameters for the case of a bi-harmonic driver with $m = 2$.

In Fig. 7 we report $\langle v \rangle$ as a function of α for different values of system parameters. Note that the curves display similar behaviors, with a resonance peak in the under-damped regime and a quick decay to zero at higher damping. This behavior is similar to the one reported in Ref. [13] for soliton ratchets in asymmetric potentials, and suggests a possible common mechanism of the phenomenon (see below). We also remark that the interruptions of the curves (cut-offs) at small α values are due to the disappearance of the kink as a consequence of the onset of spatio-temporal chaos in the system (the cut-offs delimit the borders of the existence diagram of the kinks).

Panel (a) of Fig. 7 shows the dependence of $\langle v \rangle$ on α for different values of the driving frequency. Note that the velocity is influenced by resonances with the plasma frequency and its harmonics, as one can see from the non-monotonous behavior of the cut-offs at small α (the cut-off velocities in this case have their largest values close to $\omega = 0.5$ and $\omega = 1$).

Another interesting property emerging from this figure is that the kink velocity is enhanced at low frequencies, and the average velocity decreases by increasing the frequency (already for frequencies above $\omega = 1$ directed motion is hardly visible). This is a consequence of the kink inertia to react to fast oscillations. On the contrary drift velocities are observable also at quite small values of ω (at very small values, however, the dynamics becomes complicated and requires long computational times - we checked explicitly the case $\omega = 0.01$ for which an average drift is still visible). The dashed lines in the figure represent the results of the point particle perturbation analysis of the previous section. We see that the agreement, although qualitatively reasonable, is not so good from a quantitative point of view.

In panel (b) of Fig. 7 the dependence of $\langle v \rangle$ on α is reported for different driver amplitudes (for simplicity we have varied E_1 , fixing the ratio $E_2/E_1 = 0.65$). We observe a situation similar to the one shown in Fig. 7a. By increasing the driver amplitude the system reaches the chaotic regime and cut-off values in α quickly appear. The resonant peak in this case is quite weak and visible only for some narrow range of driving amplitudes. Also here the predictions of the point particle perturbation theory are quantitatively quite poor. In the panel (c) of Fig. 7 we have shown the dependence $\langle v \rangle(\alpha)$ for different values of the relative phase θ . We see that by changing θ one can change a maximum of the curve at a given value of α , into a minimum. This is a consequence of the sinusoidal dependence of the average velocity on θ predicted in the previous section. To show this, we have reported in the inset of the figure $\langle v \rangle$ versus θ for a fixed value of α , as computed from direct numerical integrations of the sine-Gordon system. We see that the numerical points are well fitted by a sinusoidal law as expected from the first order perturbation result of the previous section. We remark that a similar sinusoidal dependence was also found in Ref. [4] for single ODE ratchets, this confirming the existence of a point-particle contribution to the effect. In experimental situations in which the relative phase between the two drivers is not accessible, one should consider θ as a random variable, and a final average on it should be taken. The above results then imply that no drift velocity can exist in these cases (soliton ratchets can be induced only if the relative phase θ remains constant in time).

It is also interesting to note from Fig. 7c that reversal currents can be induced by changing the relative phase. In Fig. 8 we show how the curve $\theta = \pi$ of Fig. 7c, (which display current reversal at low damping), changes as the driving amplitude is increased. We see that by increasing the amplitude of the driver the kink velocity is increased, this leading to an upwards shift of the curve. This means that current reversal observed for some value of θ can be removed by properly adjusting the driving amplitude (and vice-versa). Note that a further increase of the amplitude can change the shape of the curve destroying the resonant-like character.

In Fig. 9 we report the dependence of the average velocity on the driver amplitude E_1 with the ratio E_2/E_1 fixed to 0.65, and with the relative phase between the two drivers $\theta = 1.61$. From this figure it is clear that the kink drift velocity depends non linearly on the driver amplitude E_1 , with an almost cubic law as one can see from the $\log - \log$ plot in the inset. This result is in good qualitative agreement with our perturbation analysis (note that the $E_1^2 E_2$ dependence in Eq. (14) implies a E_1^3 dependence if one fixes the ratio E_1/E_2 , as done in the numerical simulations). We remark, however, that the case $\omega = 0.11$, denoted by * in Fig. 9, indicates a deviation from this law at higher values of E_1 .

We also checked the predictions of point particle symmetry arguments and perturbation theory for the case of

bi-harmonic forces with odd harmonic mixing. In Fig. 10 the dynamics of a kink driven by a bi-harmonic force with $m = 3$ is reported. In contrast with the prediction of the previous section, we see that kink can acquire a drift velocity also in this case. The direction of the motion, however, depends not only on the relative phase, but also on the initial phase (or initial time) of the driving force. By changing the initial phase we can achieve soliton moving in the opposite direction with the same velocity, thus by averaging on the initial phase one gets a zero mean velocity for the kink [simulations of the kink dynamics with different initial phases in the interval $[0, T[$ show that roughly half of that interval of initial points yield attraction to kink solutions moving to the right, the other half leading to kink solutions moving to the left with the same velocity]. A similar study for the case of $m = 2$ did not show any dependence on the initial phase or on initial time. Due to the sensitivity on initial conditions, we conclude that the kink motion in the case $m = 3$ is not related to the ratchet phenomenon (this is similar to the cases reported in Refs. [19,20]).

The net motion observed for the $m = 3$ case for fixed values of the initial phase, however, is an interesting phenomenon to explore by itself, since it is not linked with point-particle features of the soliton dynamics (these are excluded by the results of the first order perturbation theory), and is entirely related to the soliton-phonon interaction in a similar way as discussed in Ref. [13].

From the above analysis the following conclusions can be drawn. Although first order perturbation theory captures some qualitative feature of soliton ratchets, it does not provide a satisfactory description of the phenomenon. This is clear both from the fact that there is a poor quantitative agreement between the PDE results and first order perturbation analysis in the case of $m = 2$, and from the fact that for $m = 3$ it fails to predict the existence of a drift velocity depending on an initial phase. The reason for this discrepancy is that this analysis includes only point-particle aspects of the soliton dynamics, ignoring completely the internal structure of the soliton. In analogy with the mechanism described in Ref. [13], one could expect a strong contribution to transport coming from the soliton-phonon interaction. Since this interaction arises only at second order in a perturbation expansion, this explains why first order calculations fail to capture the phenomenon.

To elucidate the mechanism underlying soliton ratchets it is useful to investigate the kink dc motion in more details. In Fig. 11 we depict the kink profile while executing the ratchet dynamics in the case of a $m = 2$ driver. From this figure the existence of an internal oscillation (internal mode) of the kink profile is clearly seen. Note that the internal mode is strongly de-symmetrized with respect to the center of the kink. In the panel (a) the kink moves from the left to the right and the mode appears behind the kink. We checked that the motion of the kink is locked to the external drive. This can be seen from Fig. 11b, which shows the kink dynamics during

two periods of the driving force $E(t)$. This is in agreement with the results of Ref. [13]. The last panel, (c), shows the profile of the kink while moving in opposite direction than the one in panel (a). Note that when the kink moves to the left, the internal mode is on the right side from the kink center, so it is again behind the kink. This result indicates that there is an evident contribution to the directed kink motion hidden in the asymmetric character of the internal mode and in its interaction with the kink center of mass. We also checked that by increasing the damping the internal mode become smaller and smaller and almost disappears in the over-damped limit. This correlates with the numerical results showing the mean velocity of the kink rapidly decreasing with the increasing of the damping.

It is worth to note that although there are no internal modes frequencies in the spectrum of the small oscillation problem around exact soliton solutions of the pure sine-Gordon equation, these can arise from the perturbation field ϵf when it is switched on. This makes the proposed internal mode mechanism for soliton ratchets quite general.

Let us now briefly investigate the influence of a white noise on the kink ratchet dynamics. In Fig. 12 we report the contour plot for the kink motion in the case of a bi-harmonic driver with $m = 2$. We see that the noise introduces disturbances on the profile but does not destroy the drift motion of the soliton. We checked that this property remains true also if we increase the amplitude of the noise up to the kink-anti-kink nucleation limit. Moreover, the existence of the phenomena in presence of noise shows the validity of the above mechanism also for the non-deterministic soliton ratchets.

III. BOUNDARY EFFECTS ON SOLITON RATCHETS

In this section we discuss the effects of the system boundaries on the ratchet dynamics. We have solved the problem for two types of boundary conditions: free ends $u_x(0, t) = u_x(L, t) = 0$ and periodic boundary conditions $u(0, t) = u(L, t) + 2\pi n$, $n = \pm 1$, where L is the length of the sample. The behavior of kink and anti-kink solutions does not differ for both cases except, of course, for the behavior at the boundaries. For free boundaries one can show by perturbation theory that the kink may be destroyed at the boundaries if its incoming kinetic energy is below a certain threshold. This can be easily understood since at the boundary the kink undergoes a large-amplitude oscillation which, in presence of damping, expose the kink to larger dissipation (the oscillation will be damped and the kink will not be able to attain the -2π value and get reflected as anti-kink). The synchronization of the soliton motion with the external ac field, as well as, the fact that kink and anti-kink ratchet move in opposite directions, can allow sufficiently energetic soliton ratchets to overcome reflections in presence

of damping. This is clearly shown in Fig. 13a where a kink-anti-kink ratchet reflection is shown. The possibility to overcome reflection, however, requires, to overcome a critical energy threshold which depends on the system parameters. In Fig. 13b we show the case in which the soliton ratchet is destroyed at the boundary. At low damping the collision of the kink with the boundary generate oscillations which decay, after some time, leading to the destruction of the kink (increasing the damping the decay time quickly decreases). The possibility of overcoming reflection depends also on the relative phase of the driver and the internal mode oscillation on top of the kink (this dependence can be tested by shifting the initial incoming positions of the kink). In general, besides kink-anti-kink reflections and kink destructions, more complicated phenomena can arise, These including the possibility, for particular values of damping, amplitudes and driver frequencies, to sustain a standing breather at the boundary for very long time. Similar phenomena were also observed in Ref. [26].

To avoid the possibility of ratchet destruction at the boundaries one can recourse to periodic boundary conditions. In this case soliton ratchets, once established, will go on forever (we have checked this numerically for very long computation times). This opens the possibility of interesting physical applications as we will discuss at the end of the next section.

IV. CONCLUSIONS

In this paper we have considered a new way to produce a directed motion of a topological soliton in presence of damping, by using suitable ac drivers of zero mean. In particular we showed the possibility of establishing a ratchet dynamics for a kink of the damped sine-Gordon equation when a periodic force, consisting of two harmonic drivers, is applied. In contrast to previous works, the observed dc motion does not require any asymmetry in the potential of system, this making the phenomena easily accessible to experimental situations.

We also showed that a first order perturbation analysis based on collective coordinates does not provide a complete description of the phenomenon. The reason for this failure was ascribed to the soliton-phonon interaction which, in a perturbation analysis, appears only at second order. In particular we showed that the soliton-phonon interaction manifests with the excitation of an internal mode on the soliton profile which, in presence of damping, can interact with its translation mode. This provides a basic mechanism to convert the energy of the ac field into direct motion for the soliton which is valid for a wide class of under-damped or moderately damped nonlinear systems. Numerical simulations of the sine-Gordon equation confirm the validity of the proposed mechanism. We also investigated the influence of boundary conditions on the ratchets dynamics in finite sine-

Gordon systems. For reflective boundaries we showed the possibility for soliton ratchet to overcome reflections in presence of dissipation (for periodic boundary conditions the soliton ratchet, once established, will, obviously, go on forever). Finally, we showed that the phenomenon of soliton ratchet is robust enough to overcome the presence of the noise in the system.

This results open the possibility of interesting applications in different fields. In the context of Josephson junctions, for example, one can predict the existence of a zero field step (i.e. steps in the current-voltage characteristic related to the resonant fluxon motion in the junction) in absence of dc bias current and in presence of only bi-harmonic fields of zero average. This effect should be best observable in annular Josephson junctions where no boundary problems (kink destruction) exist. We also remark that “fluxon-ratchets” inducing zero field steps in Josephson junctions, have not yet been considered both theoretically and experimentally (we will investigate this problem in more details in a forthcoming paper).

Similar transport phenomena can be predicted also in a variety of physical systems such as dislocations in crystals, spins waves in magnetic chains, etc. Adjusting the relative phase of the drivers one could control the direction and the velocity of these excitations, this providing a way to control their dynamics. We hope that the results of this paper will soon stimulate experimental work in these directions.

V. ACKNOWLEDGEMENTS

It is a pleasure to thank P. L. Christiansen, J.C. Eilbeck, S. Flach, Y.S. Kivshar, A. C. Scott, and M.R. Samuelsen for interesting discussions. MS wishes to thank the MURST for partial financial support through the PRIN-2000 Initiative, and the Department of Physics of the Technical University of Denmark, for a two month Visiting Professorship during which this work was started. YZ acknowledges the hospitality received at the Physics Department of the University of Salerno, where part of this work was done. Both authors acknowledge partial financial support from the European Union grant LOCNET project no. HPRN-CT-1999-00163.

[1] R. Z. Sagdeev, D. A. Usikov, and G. M. Zaslavsky, *Non-linear physics : from the pendulum to turbulence and chaos*. (Harwood Academic Publ., 1992).
 [2] P. Hänggi and R. Bartussek, in: *Nonlinear Physics of Complex Systems - Current Status and Future Trends*, J. Parisi, S. C. Müller, W. Zimmermann (Eds), *Lecture notes in physics* 476, p.294 (Springer, Berlin 1996); F. Jülicher, A. Ajdari and J. Prost *Rev. Mod.*

Phys., **69** (1997) 1269; P. Reimann, *Brownian motors: Noisy Transport Far from equilibrium*, *cond-mat/0010237* (2000).
 [3] S. Flach, O. Yevtushenko and Y. Zolotaryuk, *Phys. Rev. Lett.* **84**, 2358 (2000).
 [4] O. Yevtushenko, S. Flach, Y. Zolotaryuk and A. A. Ovchinnikov, *Europhys. Lett.* **54**, (2001) 141.
 [5] S. Denisov and S. Flach, arXiv: **nlin/0104006**, 2001, to appear in *Phys. Rev. E*.
 [6] M. Barbi and M. Salerno, *Phys. Rev. E* **E 62**, (2000) 1988.
 [7] M. Barbi and M. Salerno, *Phys. Rev. E* **63**, (2001) 066212.
 [8] P. Jung, J. G. Kissner and P. Hänggi, *Phys. Rev. Lett.* **76**, (1996) 3436.
 [9] F. Marchesoni, *Phys. Rev. Lett.* **77**, (1996) 2364.
 [10] A. V. Savin, G. P. Tsironis and A. V. Zolotaryuk, *Phys. Lett. A* **229**, (1997) 279; *Phys. Rev. E* **56**, (1997) 2457.
 [11] E. Goldobin, A. Sterck and D. Koelle, *Phys. Rev. E* **63**, (2001) 031111; G. Carapella, *Phys. Rev. B* **63**, (2001) 054515.
 [12] F. Falo, P. J. Martínez, J. J. Mazo and S. Cilla, *Europhys. Lett.* **45**, (1999) 700; E. Trías, J. J. Mazo, F. Falo and T. P. Orlando, *Phys. Rev. E* **61**, (2000) 2257.
 [13] M. Salerno and N. R. Quintero, *Soliton ratchets*, submitted to *Phys.Rev.E*. 2001, arXiv:**cond-mat/0107011**.
 [14] G. Costantini and F. Marchesoni, *Phys. Rev. Lett.* **87**, (2001) 114102.
 [15] K. Seeger and W. Maurer, *Solid State Commun.*, **27** (1978) 603; I. Goychuk and P. Hänggi, *Europhys. Lett.*, **43** (1998) 503; K. N. Alekseev *et al*, *Phys. Rev. Lett.*, **80** (1998) 2669; K. N. Alekseev and F. V. Kusmartsev, **cond-mat/0012348** and references therein.
 [16] M. Salerno, *Phys. Rev. B* **44** (1991) 2720; G. Filatrella, G. Rotoli, M. Salerno, *Phys. Lett. A* **178** (1993) 81; M. Salerno, M.R. Samuelsen, *Phys. Lett. A* **190** (1994) 177.
 [17] M. Salerno and A. C. Scott, *Phys. Rev. B* **26**, (1982) 2474.
 [18] Y. S. Kivshar and B. A. Malomed, *Rev. Mod. Phys.*, **61** (1989) 763.
 [19] O. H. Olsen and M. R. Samuelsen, *Phys. Rev. B*, **28** (1983) 210; N. R. Quintero, A. Sánchez and F. G. Mertens, *Phys Rev. E*, **62** (2000) R60.
 [20] N. R. Quintero and A. Sánchez, *Eur. Phys. J.*, **B6** (1998) 133.
 [21] G. Filatrella, B. A. Malomed, R .D. Parmentier, *Phys. Lett. A*, **198** (1995) 43; experimental observation has been reported in A. V. Ustinov and B. A. Malomed, *Phys. Rev. B*, **64** (2001) 020302(R).
 [22] A. L. Sukstanskii and K. I. Primak, *Phys. Rev. Lett.*, **75** (1995) 3029; see also the related comment by Y.S. Kivshar *et al.*, *Phys. Rev. Lett.* **77** (1996) 582.
 [23] Stimulated by the results of this paper, S. Flach *et al.* have recently provided a general symmetry analysis for soliton ratchets (see arXiv:**nlin/0110013**).
 [24] D. W. McLaughlin and A. C. Scott, *Phys. Rev. A*, **18** (1978) 1652.
 [25] Directed dc motion in a nonlinear dissipative system of type (11) for a particle moving under the influence of additive bi-harmonic driver was also studied by A. K. Vidy-

bida, A. A. Serikov, in *Phys. Lett. A*, **108** (1985) 170.

[26] P. S. Lomdhal, M. R. Samuelsen, *Phys. Rev. A*, **34** (1986) 664.

Figure captions

FIG. 1. Profiles of the bi-harmonic driver for $m = 2$ (continuous line) and $m = 3$ (dashed line) for parameter values $E_1 = 0.4$, $E_2 = 0.26$, $\omega = 0.25$, $\theta = 0$. For a better comparison, a time shift of 4.548 and of -2π was respectively applied to $m = 2$ and $m = 3$ cases.

FIG. 2. Time dependence of the velocity $v(t)$ of the kink center of mass (thick dashed curve). The continuous line denote the force profile, while the dotted-dashed and dashed curves represent the response to the single dark and light pulses, respectively. The parameters are the same as in Fig. 1 with $m = 2$ and $\alpha = 0.15$.

FIG. 3. Trajectories of the kink center of mass derived from Eq. (11) for the cases $m = 2$ (continuous curve) and $m = 3$ (dashed curve). The other parameters are: $\omega = 0.25$, $\alpha = 0.1$, $E_1 = 0.4$, $E_2 = 0.26$ and $\theta = 1.61$.

FIG. 4. Average velocity $\langle v \rangle$ of the kink center of mass versus the the relative phase θ for the same parameters as in in Fig. 3. The continuous curve refers to the approximating function $\langle v \rangle = 0.058 \sin(\theta - 0.8)$.

FIG. 5. Contour plots of the velocity field $u_x(x, t)$ with $\alpha = 0.12$, $\omega = 0.25$, $\theta = 1.61$, in the cases (a) $E_1 = 0.4$, $E_2 = 0.26$ and (b) $E_1 = 0.66$, $E_2 = 0$.

FIG. 6. Contour plot of the velocity field $u_x(x, t)$ of the anti-kink motion. System parameters are as for Fig. 5a.

FIG. 7. The averaged kink velocity as a function of damping constant α with $E_2/E_1 = 0.65$ for different system parameters.

Panel (a): $E_1 = 0.4$, $\theta = 1.61$; $\omega = 0.11$ (\square), $\omega = 0.25$ (\diamond), $\omega = 0.35$ (\bullet) and $\omega = 0.65$ (\circ).

Panel (b): $\omega = 0.35$, $\theta = 1.61$; $E_1 = 0.5$ ($*$), $E_1 = 0.4$ (\bullet), $E_1 = 0.38$ (\square), $E_1 = 0.3$ (\diamond), $E_1 = 0.2$ ($+$) and $E_1 = 0.1$ (\circ).

Panel (c): $\omega = 0.25$, $E_1 = 0.4$; $\theta = 0$ (\circ), $\theta = 0.8$ (\diamond), $\theta = 1.2$ (\square) and $\theta = \pi$ ($*$).

The dashed lines show results obtained from numerical solution of Eq. (11) for $\omega = 0.11$ and $\omega = 0.25$ in (a); for $E_1 = 0.4$ in (b) and for $\theta = 0$ in (c).

The inset shows the dependence of the average velocity on the “delay angle” θ for $\alpha = 0.15$ and the rest of parameters as in Fig. 7c. The dashed curve in the inset shows the fitting curve (see text for details).

FIG. 8. Dependence of the averaged velocity $\langle v \rangle$ on damping for parameters as in Fig. 7c but with different amplitudes: $E_1 = 0.4$ ($*$), $E_1 = 0.45$ (\circ) and $E_1 = 0.5$ (\diamond). The ratio E_2/E_1 has been kept constant, $E_2/E_1 = 0.65$.

FIG. 9. The averaged kink velocity as a function of the driver amplitude E_1 with $E_2/E_1 = 0.65$, $\theta = 1.61$. The rest of the parameters were fixed as: $\omega = 0.11$, $\alpha = 0.15$ (*); $\omega = 0.35$, $\alpha = 0.15$ (\diamond); $\omega = 0.35$, $\alpha = 0.1$ (\circ); $\omega = 0.35$, $\alpha = 0.05$ (\square). The inset shows the log-log dependence.

FIG. 10. Contour plot of the velocity field $u_x(x, t)$ for a sine-Gordon kink driven by a bi-harmonic force with $m = 3$. System parameters are as for Fig. 5a except $\alpha = 0.15$ and $\theta = \pi$.

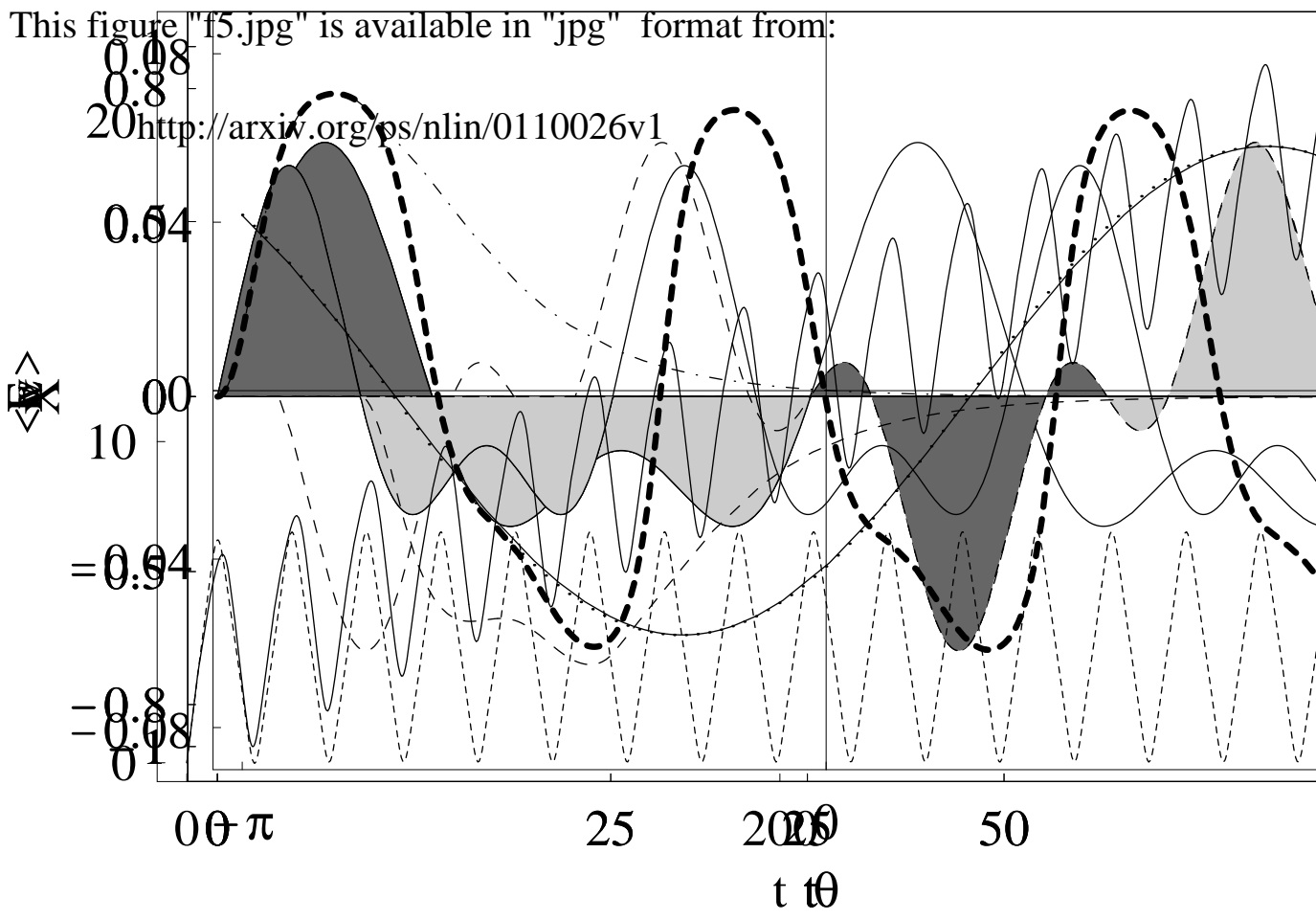
FIG. 11. Kink profile and dynamics for $\alpha = 0.15$, $\omega = 0.35$, $E_1 = 0.5$, $E_2 = 0.325$, $\theta = 1.61$ (a,b) and $\theta = 1.61 - \pi = -1.53$ (c). The profile has been computed at the time moment $t = 600$. The dashed line shows the profile of the kink after one period of the external drive.

FIG. 12. Countour plot for the displacement field $u(x, t)$ for parameters as in Fig. 1a and noise amplitude $D = 0.1$.

FIG. 13. Contour plots of kink (a) reflection and (b) annihilation at the boundary. the system parameters are $\omega = 0.11$, $E_1 = 0.4$, $E_2 = 0.26$, $\theta = 1.61$. The damping parameter was $\alpha = 0.08$ for the case (a) and $\alpha = 0.12$ for the case (b). The inset shows the anti-kink profile after reflection at time $t = 3200$.

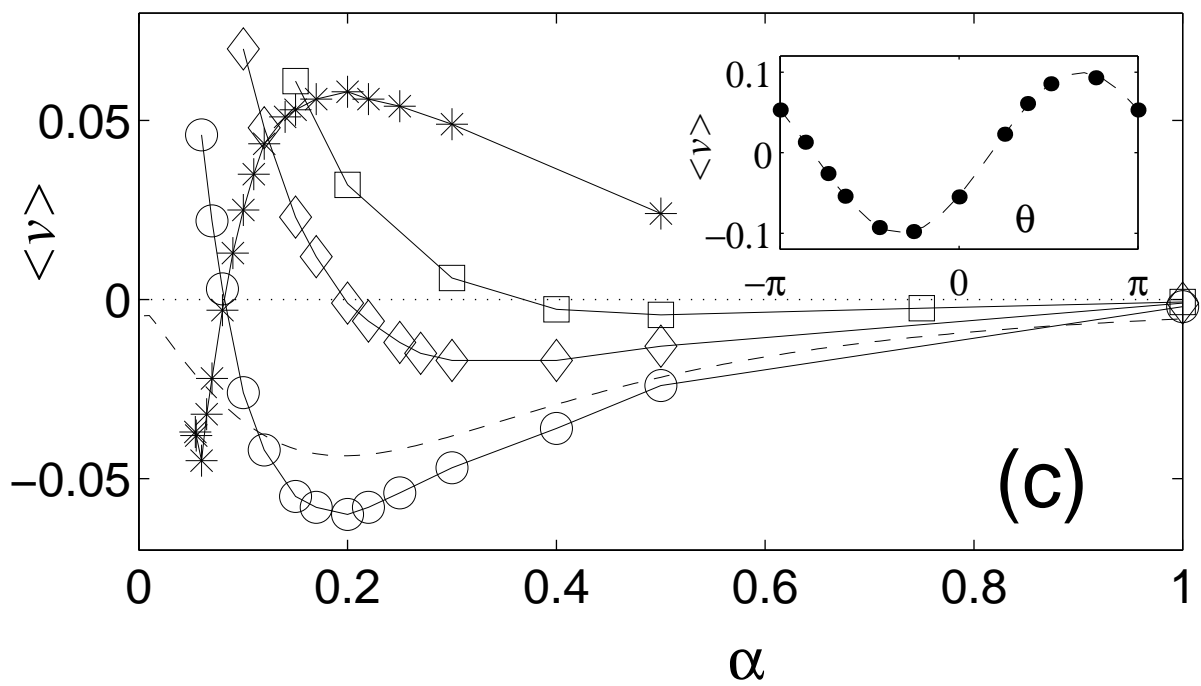
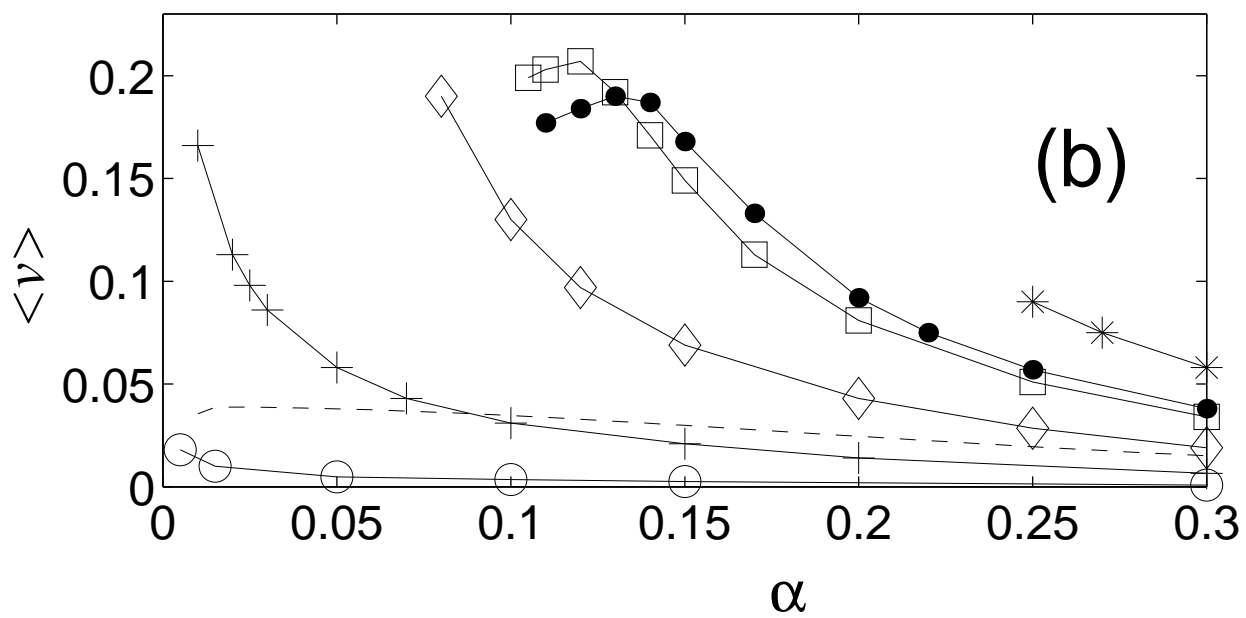
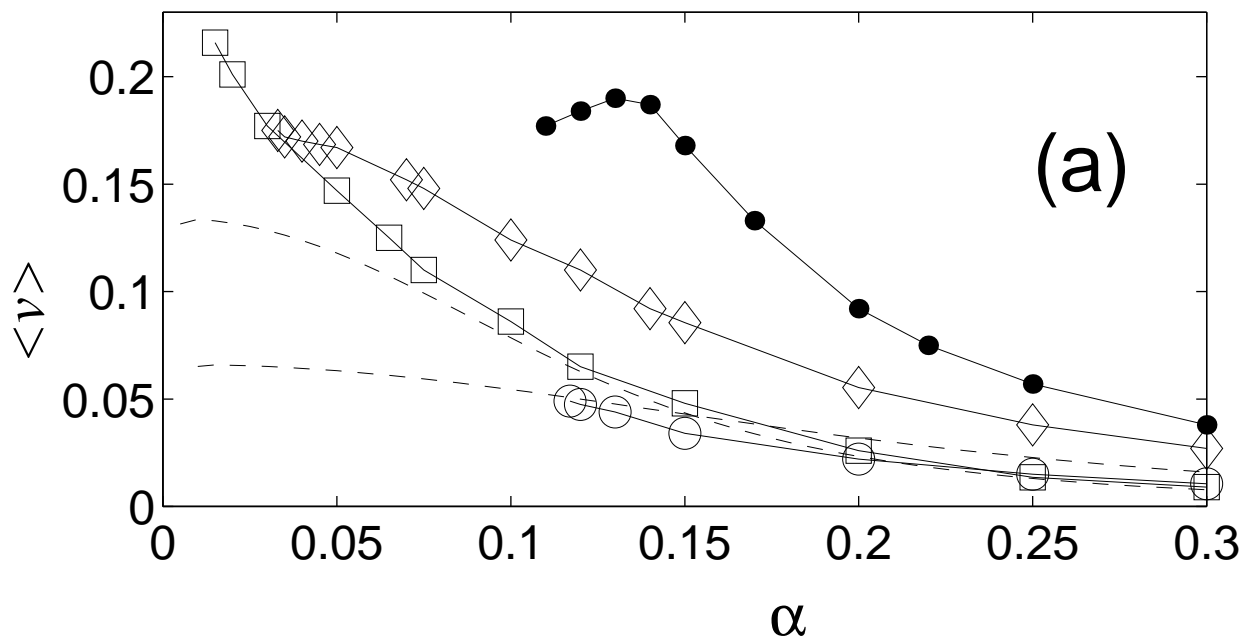
This figure "f5.jpg" is available in "jpg" format from:

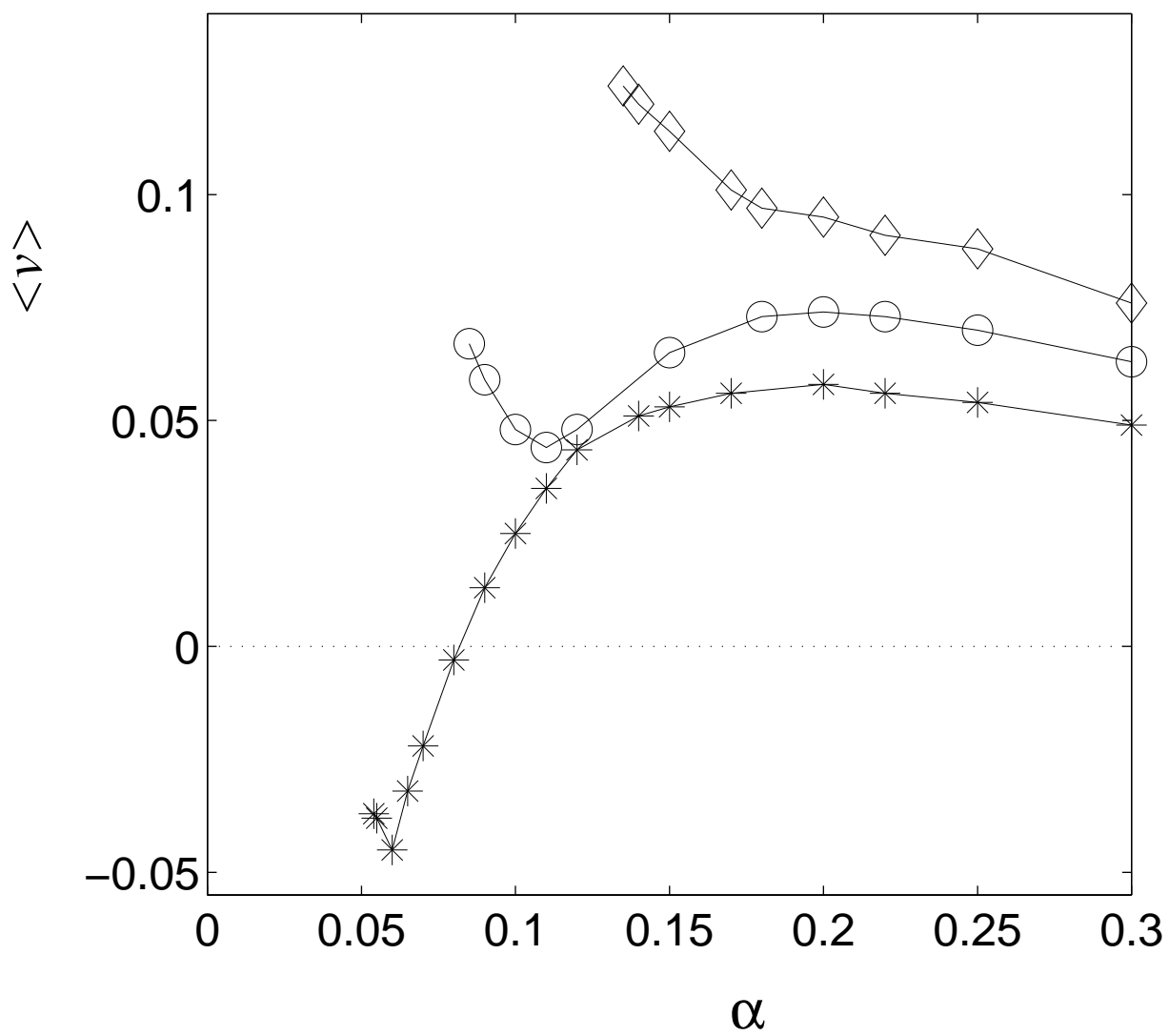
<http://arxiv.org/ps/nlin/0110026v1>

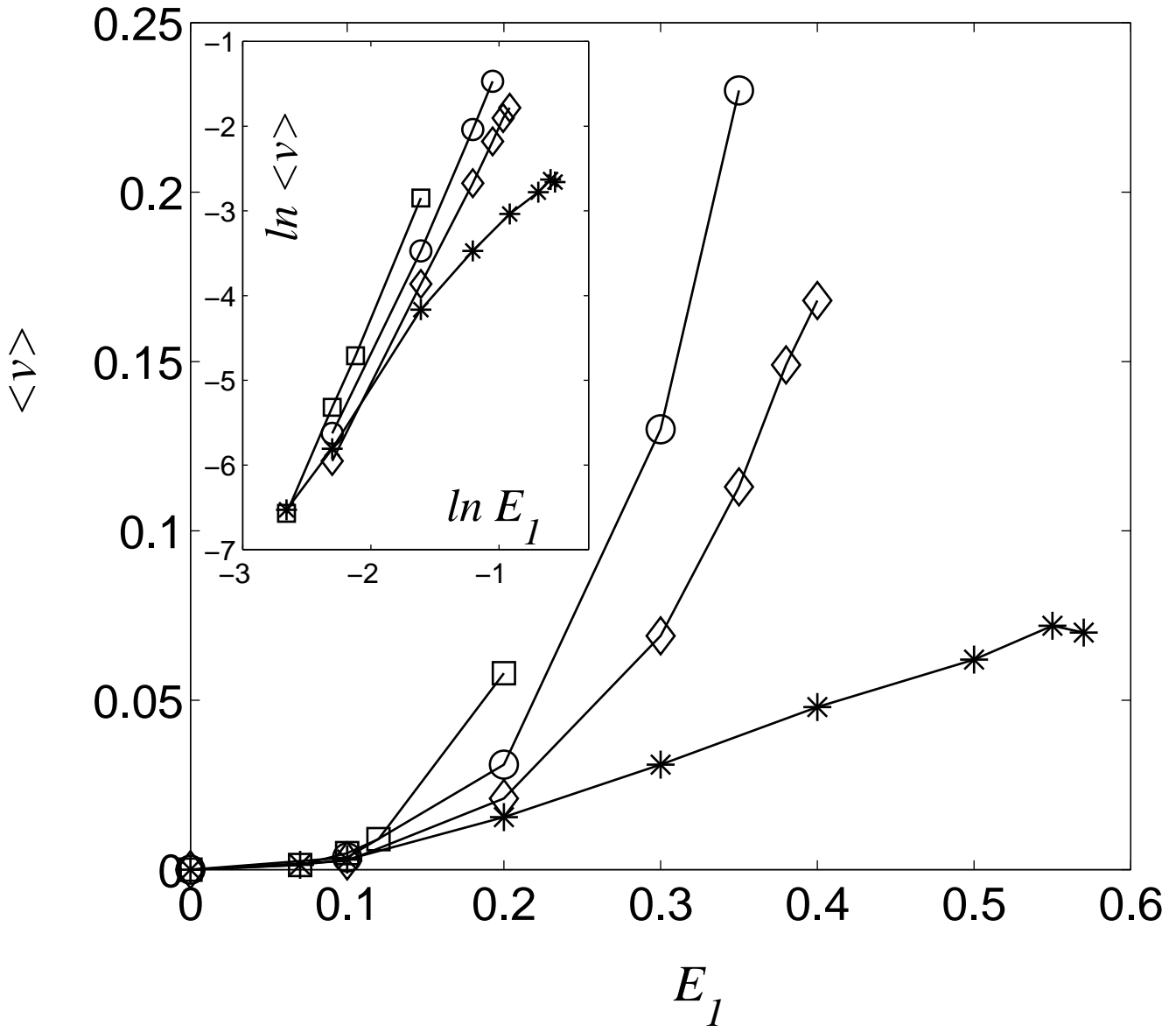


This figure "f6.jpg" is available in "jpg" format from:

<http://arxiv.org/ps/nlin/0110026v1>





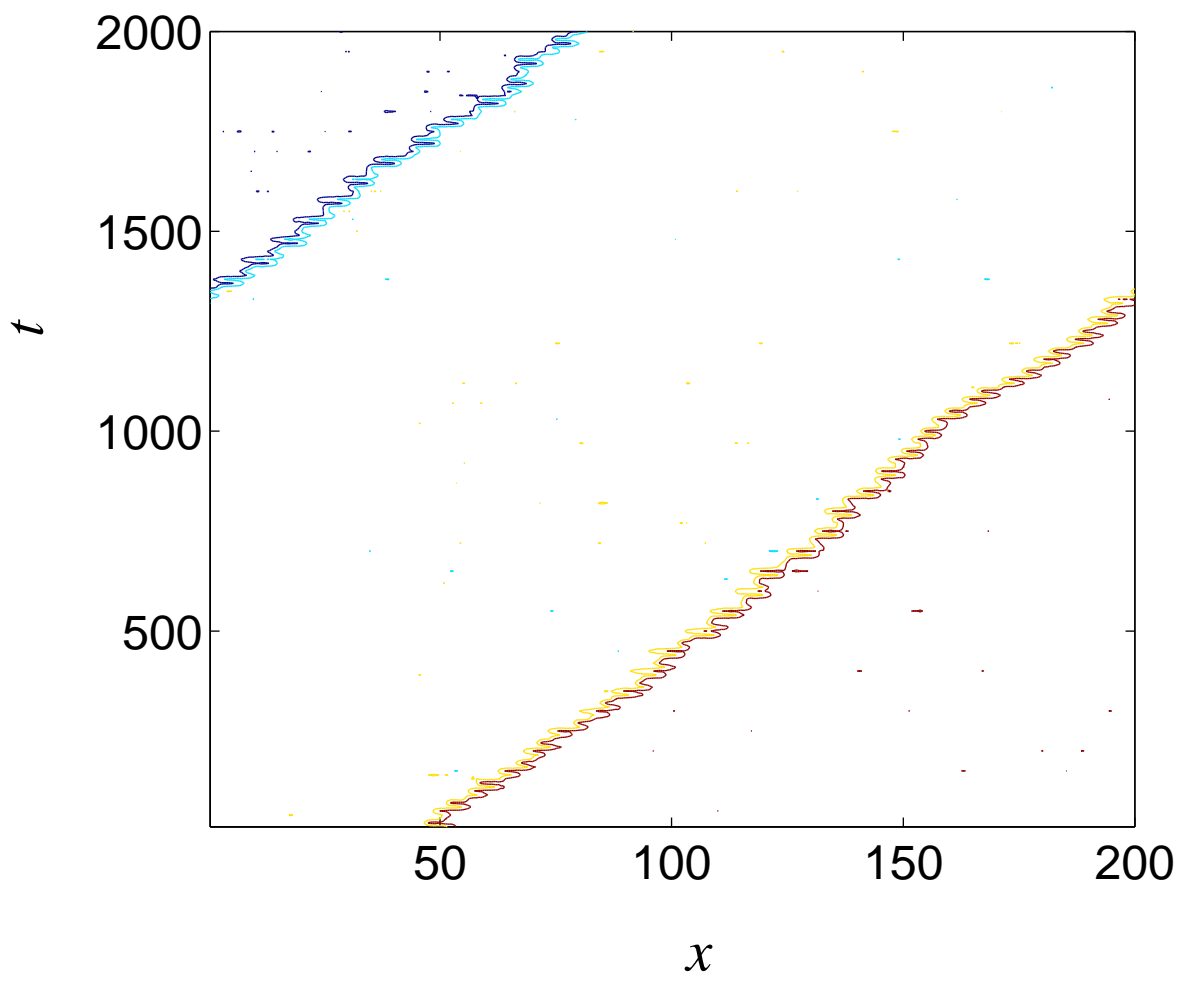


This figure "f10.jpg" is available in "jpg" format from:

<http://arxiv.org/ps/nlin/0110026v1>

This figure "f11.jpg" is available in "jpg" format from:

<http://arxiv.org/ps/nlin/0110026v1>



This figure "f13.jpg" is available in "jpg" format from:

<http://arxiv.org/ps/nlin/0110026v1>